

17th CIRP Conference on Modelling of Machining Operations

# Optimization of complex cutting tools using a multi-dexel based material removal simulation

B. Denkena<sup>a</sup>, T. Grove<sup>a</sup>, O. Pape<sup>a\*</sup>

<sup>a</sup>*Institute of Production Engineering and Machine Tools, Leibniz Universität Hannover, An der Universität 2, 30823 Garbsen, Germany*

\* Corresponding author. Tel.: +49-511-762-18259; fax: +49-511-762-5115. E-mail address: [pape@ifw.uni-hannover.de](mailto:pape@ifw.uni-hannover.de)

## Abstract

Multi-dexel based material removal simulations provide a fast and flexible way to compute process forces and tool deflections for milling and turning operations. This allows an advanced process planning including detection of collisions for complex toolpaths. However, using dexel simulations for designing cutting tools has rarely been investigated. Especially the position of individual cutting edges is not considered, because current approaches only subtract the sweep volume of the tool envelop instead of the rake face. This paper presents a new method to design cutting tools using material removal simulations and a detailed tool geometry representation. The discretization of the tool allows an efficient calculation of the engagement conditions of individual cutting edges. The method is used to optimize novel porcupine milling cutters with round indexable inserts, which produces a geometry analogous to serrated end mills. Based on the calculated forces, the positions of individual indexable inserts are adjusted to minimize the maximum radial force. An optimum has been found that reduces radial force by 12% compared to conventional porcupine milling cutters with squared inserts.

© 2019 The Authors. Published by Elsevier B.V.

Peer-review under responsibility of the scientific committee of The 17th CIRP Conference on Modelling of Machining Operations

*Keywords:* simulaton; geometric modeling; optimization

## 1. Introduction

To maximize the productivity of milling processes, special tools are increasingly being used. The geometry of the cutting edges of these tools is specially adapted for a specific application. Examples are serrated endmills to increase material removal rate during roughing [1] of form milling cutters that directly produce the final workpiece geometry. However, compared to conventional endmills, it is often difficult or even impossible to derive analytical equations for the tool-workpiece-contact area as well as the process forces.

To overcome this drawback, numerical simulations in time-domain are carried out. Compared to analytical approaches, these simulations are more flexible regarding arbitrary tool geometries and complex five-axis milling kinematics [2]. The so-called material removal simulations can be categorized

based on the discretization of the workpiece with dexel, voxel and constructive solid geometry (CSG). One example of a CSG based milling simulation is the approach of Surmann et al. [3, 4]. It describes the workpiece by a series of Boolean operations such as addition, difference and intersection. The cross section of the uncut chip is derived from the intersection volume of the tool envelope and workpiece. The major drawback of this model is the increasing complexity and requirements for computing power when individual cutting edges are considered. In the voxel model, the workpiece is described by small volume elements that either contain material or are empty [5]. However, the memory requirement grows cubically with the resolution [2], so this model is rarely used. The third mentioned approach, which is also applied in this paper, is dexel-based. Here the workpiece model is described by a grid of parallel line segments, which describe the upper

and lower boundaries of the body [6]. To improve the accuracy, three redundant dixel grids that are aligned with the coordinate axes are used in the so-called multi-dixel-models [6]. The two main advantages of dixel models are the simple to calculate line-surface intersection as well as the reduced memory requirement, which grows only quadratically with the resolution [2].

However, most of the mentioned approaches only subtract the sweep volume of the tool envelop instead of the rake face, which is necessary for the optimization of complex cutting tools. Work has already been carried out on the intersection of individual cutting edges or a representation of the rake face [6, 7], but the subsequent analysis of the shape of the uncut chip is computationally intensive. Therefore, this paper presents a new approach for a computationally efficient calculation of the tool-workpiece-contact area allowing a high temporal and spatial resolution needed for tool design.

## 2. Workflow and subject of optimization

The following work consists of three different parts. First, the above mentioned new dixel-based intersection algorithm is presented. This algorithm accelerates the analysis of the tool-workpiece-contact area and enables high temporal and spatial resolution as well as efficient consideration of single cutting edges. Second, experimental cutting tests are carried out with porcupine milling cutters in order to calibrate a force model and to validate the intersection calculation algorithm. Finally, a novel tool geometry is developed and optimized using the new intersection algorithm and the force model.

### 2.1. Subject of optimization

The experimental cutting tests as well as the optimization are conducted with porcupine milling cutters (Fig. 1. (a)). These cutters are used as a reference for a novel tool geometry invented at the Institute of Production Engineering and Machine Tools (IFW) (Fig. 1. (b)) [8]. This tool uses round indexable inserts instead of rectangular ones. This leads to a geometry similar to serrated endmills mentioned above, where a reduction of the radial force compared to conventional tools is expected. However, little is known about this new tool concept and the relation between the tool-workpiece-contact area and the positions of individual inserts. Thus, this is the ideal subject for an analysis and optimization with the presented approach.

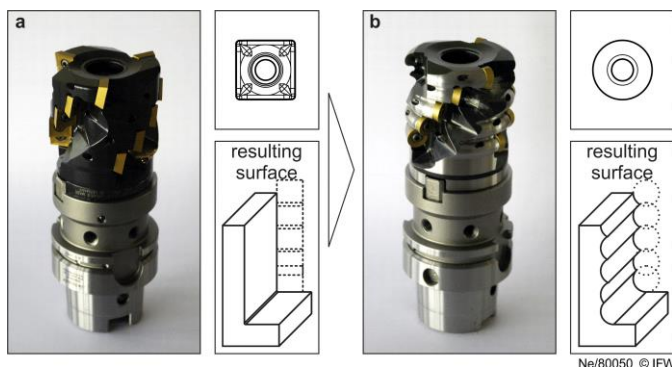


Fig. 1. (a) conventional porcupine milling cutter; (b) novel tool.

## 3. Simulation approach

As already mentioned, the approach considered in this paper is dixel-based. Therefore, the simulation consists of intersection calculations between the lines of the dexels and the surface of the tool (Fig. 2.). The envelope of all intersection points on the tool represents the cross-section of undeformed chip A. In contrast to other works, which usually describe the surface as a triangular mesh, the tools rake face is discretized with quadratic elements or quadrilaterals.

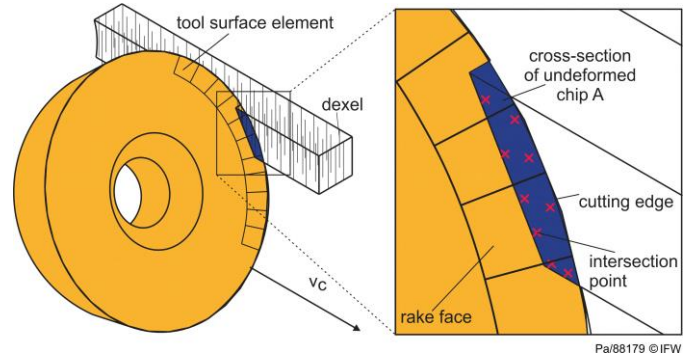


Fig. 2. Tool and workpiece discretization.

During the simulation, the quadrilaterals of the rake face are transformed with discrete time steps according to the movement of the tool. To calculate the sweep volume between two consecutive time steps, the four corners of two corresponding surface elements are also connected with quadrilaterals (Fig. 3. (a)).

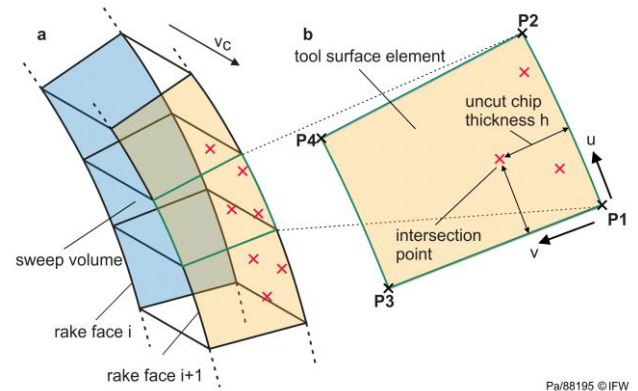


Fig. 3. (a) sweep volume generation; (b) intersection calculation

Therefore, the sweep volume consists of cubes, where each of the six bounding quadrilaterals is intersected with every dixel within the axis aligned bounding box of the element. For each dixel-quadrilateral intersection, the equation system (1) must be resolved. Here, the variables  $u$  and  $v$  ( $0 \leq u, v \leq 1$ ) are the barycentric coordinates of the quadrilateral and the vector  $\vec{D}$  contains the coordinates of the dixel.

$$\vec{D} = u(\vec{P2} - \vec{P1}) + v(\vec{P3} - \vec{P1}) + uv(\vec{P4} + \vec{P1} - \vec{P3} - \vec{P2}) \quad (1)$$

The line  $(\vec{P2} - \vec{P1})$  represents a segment of the cutting edge to which the vectors  $(\vec{P3} - \vec{P1})$  and  $(\vec{P4} - \vec{P2})$  are approximately perpendicular. The idea behind this approach is that the barycentric coordinate  $v$  is directly proportional to the

uncut chip thickness  $h$  as both point in the same direction (Fig. 3. (b)). For the calculation of the tool-workpiece-contact area, only the maximum value of  $v$  for each element needs to be found and multiplied by the distance  $|\vec{P3} - \vec{P1}|$ . This can be fully interleaved within the intersection calculation, thus reducing the computational effort by removing subsequent engagement calculations.

The force model from Altintas et al. is used for the following force calculation and given in equation [9] (2). It consists of three differential cutting forces, which are calculated for each quadrilateral. The radial force  $dF_r$  is parallel to the vector  $(\vec{P3} - \vec{P1})$  and the axial force  $dF_a$  is aligned to the vector  $(\vec{P2} - \vec{P1})$ , which corresponds to the cutting edge. The tangential force  $dF_t$  is perpendicular to both other force components. The resultant cutting forces are calculated by summarizing the incremental forces of each element. The incremental cutting edge length  $dS$  is defined equal to the length  $|\vec{P2} - \vec{P1}|$  if the quadrilateral intersects any dixel.

$$\begin{bmatrix} dF_t \\ dF_r \\ dF_a \end{bmatrix} = \begin{bmatrix} K_{tc} \cdot h \cdot dS + K_{te} \cdot dS \\ K_{rc} \cdot h \cdot dS + K_{re} \cdot dS \\ K_{ac} \cdot h \cdot dS + K_{ae} \cdot dS \end{bmatrix} \quad (2)$$

Both, the calculation of the tool-workpiece-contact area as well as the following force calculation are easy to implement and computationally inexpensive with the presented discretization using quadratic elements. Unfortunately, solving equation (1) leads to a quadratic equation that is slightly more complex than the linear equations of triangular meshes. However, this is compensated by replacing two triangles with one quadrilateral intersection. Quadratic elements also fit better in an axis aligned bounding box thus reducing the number of falsely tested dexels. The efficiency of the algorithm is demonstrated by the fact that the simulation is carried out in real time with a performance of 33,000,000 dixel intersections per second and a dixel resolution of 0.05 mm on an Intel Core i7 4790 processor.

## 4. Experimental studies

### 4.1. Experimental setup

All experimental tests were performed on a Heller H5000 machine tool using a porcupine milling cutter type M3255-050-B22-05-46 with indexable inserts of the type P4500-7461332 from Walter AG. The tool has a diameter of 50 mm and five rows with four indexable inserts each. The test material used was Ti-6Al-4V, which was attached directly to a piezoelectric force measuring device type 9255C from Kistler. During all tests, the effective spindle power was recorded directly by the machine control.

### 4.2. Design of experiments

In order to take into account the different engagement conditions between the inserts located at the face and the circumference of the tool, two different workpiece geometries were processed. Fig. 4. (a) shows the process end-milling, in which only the frontal cutting edges are engaged. In contrast to this, only the circumferential inserts are engaged in the

peripheral milling (Fig. 4. (b)). During all cutting tests, the feed rate is gradually increased to fit a suitable force model. The corresponding process parameters are given in table 1.

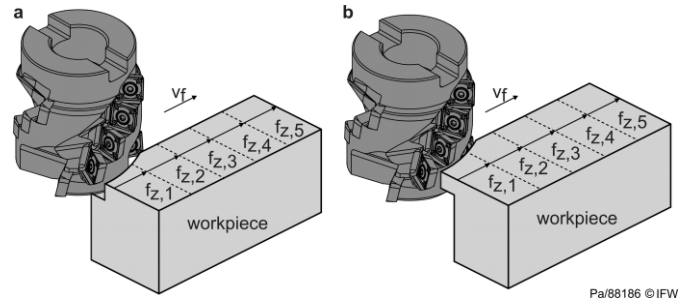


Fig. 4. (a) end-milling; (b) peripheral milling

Table 1. Variation of process parameters

Process parameter	Face milling	Peripheral milling
Axial depth of cut $a_p$	1, 3, 5, 10 mm	21 mm
Radial depth of cut $a_e$	5, 15, 30 mm	
Feed per tooth $f_z$	0.04, 0.06, 0.08, 0.10, 0.12 mm	
Cutting speed $v_c$	45 m/min	

### 4.3. Experimental verification

With the milling test of the last section, the force coefficients of equation (2) are identified mechanistically according to Gradisek et al. [10]. Therefore, all experimental cutting test are simulated with a dixel resolution of 0.025 mm and an angular step of the tool of 0.5°. To validate the mentioned force and engagement calculation, the process forces are compared in time domain (Fig. 5.). As shown in the figure, experimental and simulation results are in good agreement.

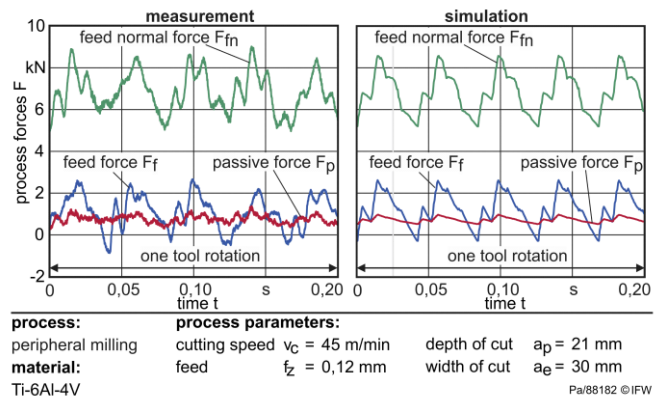


Fig. 5. Verification in time domain

In addition, the measured spindle power from the machine control minus the idling power was compared with the calculated average power of the simulation (Fig. 6.). Again, the simulation and the measurement are in good agreement. However, the measured effective power consumption is slightly higher when the process parameters increase. This is explained by higher friction in the spindle at higher forces. In summary, it can be said that the discretization with quadrilaterals and the calculation of the tool-workpiece-contact



area is suitable for the prediction of process forces for complex tool geometries.

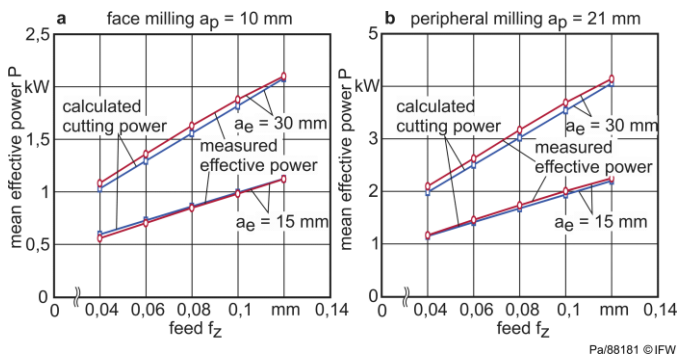


Fig. 6. (a) Verification end-milling; (b) verification peripheral milling

## 5. Optimization of the tool geometry

Based on the results of the last sections, the new tool geometry is developed and optimized. Therefore, simulations are carried out with different positions of the indexable inserts. For analysis, circular inserts with a diameter of 12 mm were selected because they are available with the same micro-geometry and carbide grade as the reference inserts. It should be mentioned that there are initially no force coefficients for this new geometry available, so the values from the reference experiments were chosen. However, the difference is expected to be small as the micro-geometry as well as the process parameters are kept constant.

For the two-dimensional optimization, the radial and angular offset between two indexable inserts was selected. The parameter range examined was based on the manufacturability of the tool body and can be found in table 2. The maximum radial force was selected as the target parameter, because the torque  $M_c = 300$  Nm and cutting power  $P_c = 9$  kW of the reference tool are not the limiting factors for the machine tool ( $M_{max} = 2292$  Nm,  $P_{max} = 60$  kW). 136 simulations were performed with an angular resolution of  $0.5^\circ$ , a dixel resolution of  $0.025$  mm, a axial depth of cut  $a_p = 40$  mm and a radial depth of cut  $a_e = 30$  mm. The results of the optimization can be found in Fig. 7. An optimum was found with an angular offset of  $36^\circ$  and an axial offset of  $7.4$  mm with a maximum radial force of  $13.1$  kN. Compared to the reference tool with a maximum radial force of  $14.9$  kN, the force was reduced by approx. 12% at the same process parameters.

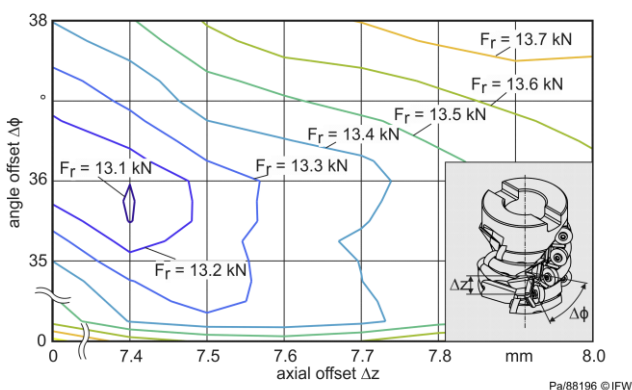


Fig. 7. Optimization of the tool geometry

Table 2. Variation of tool parameters

Tool parameter	starting value	end value	increment
Angle offset $\Delta\phi$	$34^\circ$	$38^\circ$	$0.25^\circ$
Axial offset $\Delta z$	7.3 mm	8.0 mm	0.1 mm

## 4. Conclusion

In this study, a new approach for computationally fast and efficient analysis of the tool-workpiece-contact area of discrete cutting edges has been presented and successfully validated. This algorithm has been used to analyze a novel tool geometry developed at the Institute of Production Engineering and Machine Tools (IFW). The new geometry transfers the concept of serrated endmills to porcupine milling cutters. In the following optimization step using the mentioned simulation, an optimum for the tool geometry was found and the expected reduction of the radial force was shown. The high nonlinearity of the relation between the process forces and the tool geometry shows the effectiveness of the mentioned algorithm. In further work, the found tool geometry will be manufactured and further optimized.

## Acknowledgements

The IGF-project (IGF – 19654 N WSF) of the Research Association (FGW) was supported by the AiF within the program for the promotion of industrial research (IGF) from the Federal Ministry of Economy and Energy due to a decision of the German Bundestag. The authors would like to thank the Walter AG for providing the cutting tools.

## References

- [1] Tehranizadeh F, Budak E. Design of Serrated End Mills for Improved Productivity. *Procedia CIRP*. 2017;58:493–8.
- [2] Altintas Y, Kersting P, Biermann D, Budak E, Denkena B, Lazoglu I. Virtual process systems for part machining operations. *CIRP Annals*. 2014;63(2):585–605.
- [3] Surmann T., Biermann D. The effect of tool vibrations on the flank surface created by peripheral milling. *CIRP Annals* 2008;57(1):375-378.
- [4] Surmann T, Enk D. Simulation of milling tool vibration trajectories along changing engagement conditions. *International Journal of Machine Tools and Manufacture*. 2007 Jul;47(9):1442–8.
- [5] Nishida I, Okumura R, Sato R, Shirase K. Cutting Force and Finish Surface Simulation of End Milling Operation in Consideration of Static Tool Deflection by Using Voxel Model. *Procedia CIRP*. 2018;77:574–7.
- [6] Boess V, Ammermann C, Niederwestberg D, Denkena B. Contact Zone Analysis Based on Multidixel Workpiece Model and Detailed Tool Geometry Representation. *Procedia CIRP*. 2012;4:41–5.
- [7] Erkorkmaz K, Katz A, Hosseinkhani Y, Plakhotnik D, Stautner M, Ismail F. Chip geometry and cutting forces in gear shaping. *CIRP Annals*. 2016;65(1):133–6.
- [8] Denkena B, Nesper D. Fräswerkzeug, Patent specification, German Patent and Trademark Office 2017, DE 102016104005 A1, Publication date: 07.09.2017.
- [9] Engin S., Altintas Y. Mechanics and dynamics of general milling cutters. *International Journal of Machine Tools and Manufacture* 2011;41:2195.
- [10] Gradisek J., Kalveram M., Weinert K. Mechanistic identification of specific force coefficients for a general end mill. *International Journal of Machine Tools and Manufacture* 2004;44:401-414.